Published in final edited form as:
Biochim Biophys Acta. 2009 March ; 1793(3): 489–495. doi:10.1016/j.bbamcr.2008.11.017.

A Novel Mode of Translocation for Cytolethal Distending Toxin

Lina Guerra[a], **Kathleen N. Nemec**[b], **Shane Massey**[b], **Suren A. Tatulian**[c], **Monica Thelestam**[a], **Teresa Frisan**[a], and **Ken Teter**[b,*]

a *Department of Cell and Molecular Biology, Karolinska Institutet, Stockholm, Sweden*

b *Department of Molecular Biology and Microbiology, Burnett School of Biomedical Science, College of Medicine, University of Central Florida, Orlando, Florida, USA*

c *Department of Physics, University of Central Florida, Orlando, Florida, USA*

Summary

Thermal instability in the toxin catalytic subunit may be a common property of toxins that exit the endoplasmic reticulum (ER) by exploiting the mechanism of ER-associated degradation (ERAD). The *Haemophilus ducreyi* cytolethal distending toxin (HdCDT) does not utilize ERAD to exit the ER, so we predicted the structural properties of its catalytic subunit (HdCdtB) would differ from other ER-translocating toxins. Here, we document the heat-stable properties of HdCdtB which distinguish it from other ER-translocating toxins. Cell-based assays further suggested that HdCdtB does not unfold before exiting the ER and that it may move directly from the ER lumen to the nucleoplasm. These observations suggest a novel mode of ER exit for HdCdtB.

Keywords

cytolethal distending toxin; circular dichroism; endoplasmic reticulum; fluorescence spectroscopy; 20S proteasome; toxin translocation

1. Introduction

The *Haemophilus ducreyi* cytolethal distending toxin (HdCDT) is an AB-type genotoxin that consists of a catalytic A moiety (HdCdtB) and a cell-binding B moiety (HdCdtA + HdCdtC) [1]. Like many AB toxins, HdCDT must travel from the plasma membrane to the endoplasmic reticulum (ER) before its A moiety can escape the endomembrane system to reach its target [2,3]. Translocation of the A chain from the ER to the cytosol is thought to involve the ER-associated degradation (ERAD) quality control system [4,5], but HdCDT intoxication is not inhibited by alterations to ERAD that generate resistance against five other ER-translocating toxins: *Pseudomonas aeruginosa* exotoxin A, *Escherichia coli* heat-labile toxin IIb, cholera toxin (CT), plasmid-encoded toxin, and ricin [3,6–9]. Thus, exit of HdCdtB from the ER occurs by an ERAD-independent mechanism or by an ERAD mechanism that is significantly different from the pathway utilized by many other ER-translocating toxins. HdCDT is also unique in that it must reach the nucleus in order to function whereas other ER-translocating toxins act in the cytosol.

*Corresponding author: Biomolecular Research Annex, 12722 Research Parkway, Orlando, Florida 32826. Tel: 407-882-2247 Fax: 407-384-2062 Email: kteter@mail.ucf.edu.

ERAD-mediated toxin translocation may depend upon the heat-labile nature of the isolated toxin A chain. The catalytic CTA1 polypeptide, the A subunit of pertussis toxin (PT S1), and ricin A chain are all in partially or fully unfolded states at near-physiological temperatures [10–12]. However, thermal instability is not apparent when the toxin A chain is present in a holotoxin [13–15]. A/B subunit dissociation, an event that occurs in the ER translocation site, could thus serve as the trigger for toxin unfolding. This structural shift would identify the toxin A chain as a misfolded protein and would thereby promote its ERAD-mediated export into the cytosol. Most ERAD substrates are rapidly degraded in the cytosol by the ubiquitin-26S proteasome system, but the A chains of ER-translocating toxins are thought to avoid this fate because they have a paucity of the lysine residues that serve as ubiquitin attachment sites [4]. The translocated A chains may instead be degraded by a relatively slow, ubiquitin-independent mechanism involving the core 20S proteasome [11,12,16].

The distinctive nature of the HdCDT translocation mechanism suggested that HdCdtB may not exhibit the same physical characteristics observed for the A chains of other ER-translocating toxins. To test this prediction, biophysical and biochemical experiments were performed on the purified HdCdtB protein. We found that, in contrast to the A chains of other ER-translocating toxins, HdCdtB was heat-stable and resistant to degradation by the 20S proteasome. Cell-based assays further suggested that HdCdtB does not unfold before exiting the ER and that it may move directly from the ER lumen to the nucleoplasm. These results highlight the distinctive nature of CDT and suggest the cellular processing of HdCdtB differs from host-toxin interactions involving other ER-translocating toxins.

2. Materials and methods

2.1 Biophysical studies

HdCdtB was purified from *E. coli* transformed with a glutathione S-transferase (GST)-CdtB expression vector as previously described [17]. After removal of the GST tag, biophysical measurements were performed on 0.15 mg HdCdtB in 0.2 ml 10 mM Hepes (pH 7.0) with 1 mM $CaCl_2$ as described [11]. For fluorescence measurements, the samples were excited at 280 nm and emission spectra recorded between 300 to 400 nm. For circular dichroism (CD) measurements, ellipticity, θ, was measured between 200 nm and 250 nm using a J-810 spectrofluoropolarimeter (Jasco Corp., Tokyo, Japan). After subtracting the spectra of the buffer, the mean residue molar ellipticity was calculated as $[\theta] = \theta/ncl$, where θ is the measured ellipticity in millidegrees, n is the number of residues per molecule, c is the molar concentration, and l is the optical path-length in mm. The temperature dependencies of the maximum fluorescence emission wavelengths or the ellipticities were fitted with theoretical curves as described previously [11].

2.2 Degradation assays

The protease sensitivity assay and the 20S proteasome assay were performed as previously described [11]. The CTA1/CTA2 heterodimer was purchased from Calbiochem (La Jolla, CA); thermolysin was purchased from Sigma-Aldrich (St. Louis, MO); and the 20S proteasome was purchased from Boston Biochem (Cambridge, MA).

2.3 Toxicity assays

The assay for HdCDT induction of H2AX phosphorylation was performed as previously described [18]. HdCDT was reconstituted from individual subunits as described in [3]. The 2 μg/ml concentration of HdCDT used for this assay represents the minimal amount of toxin required to elicit an effect in 100% of the cells after 2 h of intoxication. Toxicity assays with ricin (Vector Laboratories, Burlingame, CA) were based upon the toxin-induced inhibition of protein synthesis as described in [16].

2.4 Construction of CdtB-CVIM

A C-terminal extension containing the -CVIM farnesylation site was introduced into CdtB using the *cdtB* nucleotide sequence from the pGEX-CdtB-sulf1 plasmid [3] as a template. The following primers were used:

5′-ATTCGGATCCAACTTGAGTGACTTCAAAGTAGC-3′

and

5′-
TACCGAATTCTCACATGATCACACACCCAGATGGGTATTCGTAGTCTTCTGCGCT
G CGATCACGAACAAAACTAAC-3′

The PCR fragment was cloned into the *Bam*HI and *Eco*RI restriction sites of the pGEX4T3 expression vector (GE Healthcare, Piscataway, NJ). Purification of the fusion protein produced in *E. coli* strain BL21 DE3 was performed according to the instructions of the manufacturer (GE Healthcare).

2.5 Farnesylation assays

Detergent phase partitioning of lysates from cells exposed for 4 h to 50μg/ml of a CDT holotoxin containing the GST-CdtB-CVIM subunit was performed as previously described [19]. GST-CdtB-CVIM was recovered from aqueous and detergent phases of the lysates by affinity purification with glutathione sepharose 4B for 1 h at 4°C. Western blot was then performed using a horse radish peroxidase-conjugated anti-GST antibody (Novus Biologicals, Littleton, CO). In vitro farnesylation of GST-CdtB-CVIM was demonstrated by mixing 5 μg of the protein with 35 μl rabbit reticulocyte lysate (Sigma-Aldrich), 1 mM $MgCl_2$, and 5 mM farnesyl pyrophosphate (Sigma-Aldrich) for 1 h at 37°C. Detergent phase partitioning of the reaction product was performed as described in [19].

2.6 Confocal Microscopy

HeLa cells grown on coverslips were transfected with 2 μg of the pDSRed2-ER vector (Clontech, Mountain View, CA) using the Lipofectamine 2000 Reagent (Invitrogen, Carlsbad, CA) according to the manufacturer's instructions. The pDSRed2-ER vector encodes a recombinant protein consisting of a *Discosoma* sp. red fluorescent protein appended with an amino-terminal signal sequence for co-translational targeting to the ER lumen and a carboxy-terminal KDEL ER retention motif. At 24 h post-transfection, cells were exposed for 4 h to 10 μg/ml of a CDT holotoxin containing a GST-tagged CdtB subunit [17]. The cells were then fixed with 4% paraformaldehyde and permeabilized with 0.2% Triton X-100 in phosphate buffered saline for 10 min at 22°C. Non-specific antibody binding was blocked by incubation with 3% bovine serum albumin in phosphate buffered saline for 30 min at 22°C. GST-CdtB was visualized using a fluorescein-conjugated goat anti-GST antibody (Abcam, Cambridge, MA) at 1:50 dilution for 30 min at 25°C. Cells were viewed with a Nikon TE 300 confocal microscope, and images were captured using the Perkin Elmer (Waltham, MA) UltraViewERS software.

3. Results

3.1 Thermal Stability of HdCdtB

Fluorescence spectroscopy and far-UV CD were used to examine the thermal stability of HdCdtB (Fig. 1), a 29 kDa protein with ~13% α-helix content and ~40% β-sheet content [20, 21]. Measurements were conducted with buffer conditions (pH 7.0, 1 mM Ca^{2+}) that approximated the physiological conditions of the ER (pH 7.2, 0.5 mM Ca^{2+}) [22–25].

Fluorescence spectroscopy detected the solvent exposure of previously buried aromatic residues by a red shift in the maximum emission wavelength (Figs. 1A & 1B). These readings demonstrated that substantial disordering of the HdCdtB tertiary structure did not occur at 37ºC. In fact, sample heating to 60ºC was required to observe the disordering of HdCdtB tertiary structure. Near-simultaneous measurements of fluorescence and CD spectra were performed on the same HdCdtB sample in a 4 mm × 4 mm optical path-length rectangular quartz cuvette in order to reduce sample-to-sample variability. This procedure generated some noise in the far-UV CD spectra because of the relatively large optical path-length (not shown). Nevertheless, analysis of the ellipticity at 220 nm (which reflects the α-helical and β-sheet secondary structures) demonstrated that substantial denaturation of the HdCdtB secondary structure only occurred at temperatures above 50ºC (Fig. 1C). Thus, significant unfolding of HdCdtB did not occur at physiological temperature. The conformational changes that occurred at high temperatures were not completely reversible, as the red shift of the fluorescence spectra and the reduced ellipticity did not return to their initial values upon sample cooling to 18ºC (Figs. 1B & 1C).

3.2 Proteolysis of HdCdtB

The thermal stability of HdCdtB was also examined with a protease sensitivity assay (Fig. 2A). This technique is often used to probe the folding state of a protein, as properly folded proteins are generally more resistant to proteolysis than unfolded variants of the same protein [10,26–28]. To detect temperature-induced changes in the folding state of HdCdtB, toxin samples were incubated at temperatures ranging from 4ºC to 45ºC for 45 minutes. The samples were then placed on ice and incubated with thermolysin for another 45 minutes at 4ºC. Finally, EDTA and sample buffer were added to halt the proteolytic digestions. Thermolysin is a calcium-dependent metalloprotease that hydrolyzes peptide bonds on the amino side of bulky hydrophobic residues [27]. The use of this specific protease thus allowed us to detect temperature-induced conformational changes that resulted in the exposure of previously buried hydrophobic residues. For comparative purposes, parallel experiments were run with the reduced CTA1/CTA2 heterodimer. Reduction of the CTA1/CTA2 disulfide bond normally occurs in the ER of an intoxicated cell [29]; this event was reproduced in vitro by including 10 mM β-mercaptoethanol in the assay buffer. Previous work has demonstrated the complete dissociation of CTA1 from CTA2 under this reducing condition [12].

HdCdtB exhibited considerable resistance to proteolysis with thermolysin when incubated at temperatures up to 45ºC. In contrast, reduced CTA1 was completely degraded at temperatures ≥41ºC, and substantial degradation of the CTA1 sample pre-incubated at 37ºC was observed as well. Temperatures ≥33ºC also induce PT S1 to assume a thermolysin-sensitive conformation [11]. Thus, at physiological temperature CTA1 and PT S1 contain surface-exposed hydrophobic residues that could trigger the ERAD translocation mechanism. HdCdtB, in contrast, exhibited remarkable heat stability and thermolysin resistance when compared to the A chains of other ER-translocating toxins.

In vitro, reduced CTA1 and reduced PT S1 are susceptible to ubiquitin-independent degradation by the core 20S proteasome [11,12]. As the 20S proteasome only acts upon unfolded substrates [30], toxin processing by this form of the proteasome is likely linked to thermal instability in the toxin A chain. The relatively heat-stable nature of HdCdtB would therefore render it resistant to degradation by the 20S proteasome. To test this prediction, we incubated HdCdtB or the reduced CTA1/CTA2 heterodimer with the purified 20S proteasome (Fig. 2B). Little to no degradation of HdCdtB occurred during the 20 hour time frame of this experiment. In contrast, degradation of the reduced 21 kDa CTA1 polypeptide was evident at 4 hours of incubation and was nearly complete by 8 hours of incubation. Thus, HdCdtB was not an effective substrate for the 20S proteasome.

3.3 Unique Features of HdCdtB Translocation

Most proteins require at least partial unfolding in order to move from the ER to the cytosol, yet our data indicated that the isolated HdCdtB subunit is in a folded conformation at 37ºC. To examine the role of A chain unfolding in HdCDT intoxication, we performed toxicity assays with glycerol-treated HeLa cells (Fig. 3). Chemical chaperones such as glycerol prevent protein unfolding [31] and block intoxication with five distinct ER-translocating toxins: ricin [32], exotoxin A [32], plasmid-encoded toxin [33], CT, and Shiga toxin 2 (Teter et. al, unpublished observations). An inhibition of HdCDT activity in glycerol-treated cells would therefore suggest that a chaperone-assisted unfolding step may be necessary for HdCdtB to reach its target.

Toxicity assays were performed on HdCDT-treated HeLa cells incubated in the absence or presence of 10% glycerol (Fig. 3A–B). Cells were exposed to HdCDT and glycerol for a two hour co-incubation before screening for toxic effects. In parallel experiments, cells were also pre-incubated with glycerol for one hour before a two hour co-incubation with HdCDT and glycerol. Prolonged incubation with glycerol was toxic to the cells, so we could not assess HdCDT intoxication by its long-term effect of cell cycle arrest. Phosphorylation of the histone H2AX as been shown to occur early in the CDT intoxication process [18] and was therefore used as an alternative measure of intoxication. Exposure to glycerol did not prevent the phosphorylation of H2AX in HdCDT-treated cells (Fig. 3A–B), but it did block intoxication with ricin (Fig. 3C). The latter result demonstrated that our experimental procedure was sufficient to inhibit the activity of a prototypical ER-translocating toxin. Importantly, glycerol treatment alone did not result in the phosphorylation of H2AX (Fig. 3A–B). These collective observations emphasized the unusual aspects of HdCDT intoxication, a process which may not require A chain unfolding prior to translocation.

We have previously suggested that HdCdtB may bypass the cytosol and move directly from the ER to the nucleus [1,3]. This atypical translocation mechanism would be distinct from the ERAD-mediated pathway that exports heat-labile toxin A chains to the cytosol. To further examine this putative translocation route, we generated a recombinant HdCDT that contains a CVIM-tagged HdCdtB subunit. The C-terminal CVIM farnesylation motif can serve as an indicator of protein localization to the cytosol because farnesylation, which increases the hydrophobicity of the target protein, is a cytosolic modification [34]. The recombinant HdCdtB also contained an N-terminal GST tag to facilitate protein purification and detection.

A farnesylated protein will partition into the detergent phase of Triton X-114, whereas an unmodified variant of the same protein will partition into the aqueous phase. We confirmed that GST-HdCdtB-CVIM behaved in this predicted manner by performing an in vitro farnesylation assay. Purified GST-HdCdtB-CVIM partitioned into the aqueous phase of Triton X-114 (Fig. 4A, left panel). However, GST-HdCdtB-CVIM partitioned into the detergent phase of Triton X-114 when it was exposed to the farnesylation machinery present in a reticulocyte lysate (Fig. 4A, right panel). The farnesylation of GST-HdCdtB-CVIM could therefore be detected by detergent phase partitioning of the modified toxin.

For in vivo experiments, we incorporated GST-HdCdtB-CVIM into a CDT holotoxin. HeLa cells were exposed to 50 μg/ml of the recombinant holotoxin for 4 hours before cell extracts were generated with a Triton X-114 lysis buffer. As shown in Fig. 4B, GST-HdCdtB-CVIM could only be found in the aqueous phase of the cell extract. This indicated that no detectable pool of HdCdtB was modified by the cytosolic farnesylation machinery. Cells exposed to an HdCdtA/HdCdtC heterodimer or to GST-HdCdtB-CVIM alone did not produce an HdCdtB signal (data not shown). This demonstrated that the protein detected in vivo was GST-HdCdtB-CVIM and that, as expected, an intact holotoxin was required to deliver GST-HdCdtB-CVIM into the target cell. Given the robust HdCdtB signal present in the aqueous phase of the HeLa

cell extract, any trace amount of farnesylated GST-HdCdtB-CVIM would represent an exceedingly small pool of the total protein.

Methods such as Western blot analysis that directly monitor the toxin itself are less sensitive than toxicity assays and therefore require higher toxin doses for experimentation. Thus, it was necessary to use 25-fold more HdCDT for the farnesylation assay than for the toxicity assay of Figure 3. The relatively short-term intoxication periods of 2–4 hours for our in vivo experiments also required the use of high toxin concentrations. In our previous work, a 4 hour exposure to 20 μg/ml of HdCDT was required to detect sulfation and mannosylation of the recombinant HdCdtB subunit [3]. This toxin concentration did not alter the cellular responses in terms of biochemical signaling. Likewise, the 4 hour exposure to 50 μg/ml of toxin that was required for our farnesylation assay did not alter the cell morphology as determined by actin and nuclear staining. Furthermore, the cellular distension that is only seen after long-term intoxications was not observed in cells exposed to 50 μg/ml of HdCDT for 4 hours. Collectively, these observations indicated that the high toxin concentration required for our farnesylation assay did not alter the cellular response to HdCDT intoxication.

A direct ER-to-nucleoplasm translocation route would bypass the cytosolic farnesylation machinery and therefore leave HdCdtB in an unmodified state. Confocal microscopy was used to further examine this putative translocation route (Fig. 5). HeLa cells were exposed for 4 hours to 10 μg/ml of a recombinant CDT holotoxin that contained a GST-tagged CdtB subunit [17]. The cellular location of GST-CdtB was then compared to the distribution of DsRed2-ER, a fluorescent marker for the ER. GST-CdtB and DsRed2-ER could be found in a branching, tubularized network that was contiguous with the nuclear envelope (arrows). GST-CdtB could also be found in the nucleus but could not be detected in the cytosol. As with the farnesylation data, this suggested that HdCdtB bypasses the cytosol and moves directly from the ER to the nucleus. Finally, GST-CdtB and DsRed2-ER were visualized in invaginations of the nuclear envelope that protruded into the nucleus (arrowheads). These structures have been previously visualized in unintoxicated cells and are morphologically defined as the nucleoplasmic reticulum [35–37]. By visualizing DsRed2-ER in unintoxicated HeLa cells, we confirmed that the tubular protrusions were a normal cellular structure rather than a byproduct of HdCDT intoxication and that the DsRed2-ER signal did not bleed into the fluorescein channel used to visualize GST-CdtB (not shown). Localization to the nucleoplasmic reticulum (i.e., the nuclear protrusions) has not been reported for other toxins that have been visualized in the ER [19, 24,38–40]. This again emphasized the unique aspects of HdCDT intoxication. The functional relevance of these nuclear protrusions in regards to CDT intoxication has yet to be determined.

4. Discussion

CDTs are produced by numerous Gram-negative pathogens [1]. They are the only known bacterial AB toxins that function primarily by direct damage to the host cell DNA. CdtB accordingly acts within the nucleus, whereas other toxin A chains act within the cytosol. Our current study demonstrates that, in addition to its unique target and unique site of action, CdtB also exhibits unique structural properties which affect its interaction with the host cell and distinguish it from the A chains of other ER-translocating toxins.

With the exception of the *Salmonella* Typhi CDT [41], the family of CDTs are tripartite toxins composed of a cell-binding CdtA/CdtC subunit and a catalytic CdtB subunit. Both CdtA and CdtC are required for the optimal biological activity of CDT, but the two proteins do not appear to play equivalent roles in cell binding and cellular uptake [1,42–46]. Although the exact roles of CdtA and CdtC in toxin endocytosis and intracellular trafficking remain to be determined, it is well-established that CdtB must exit the endomembrane system and reach the nucleus in order to elicit a cytotoxic effect [2,3,45,47]. HdCdtB escape from the endomembrane system

occurs at the level of the ER and involves an ERAD-independent mechanism or an ERAD mechanism that is significantly different from the pathway utilized by other ER-translocating toxins [3]

Many ER-translocating toxins exploit ERAD for passage into the cytosol [4,5]. For three of these toxins - CT, PT, and ricin - thermal instability in the isolated catalytic subunit may activate the ERAD mechanism [10–12]. The heat-labile nature of the toxin A chain could also facilitate its ubiquitin-independent degradation by the 20S proteasome. Our results provide previously unknown evidence that HdCdtB maintains its folded conformation at 37ºC in buffer conditions that mimic the physiology of the ER. This offers a structural basis for the previously reported ERAD-independent mechanism of HdCdtB export from the ER [3]: since HdCdtB does not unfold at 37ºC, it is not recognized as an ERAD substrate. The thermal stability of HdCdtB also protects it from degradation by the 20S proteasome, a proteolytic machine that can only act upon unfolded proteins. Finally, CDT is the only known ER-translocating toxin that can function in glycerol-treated cells. The structural and cellular events involved with HdCdtB export from the ER are therefore distinct from those events involving other ER-translocating toxins.

The productive intoxication of glycerol-treated cells suggests that HdCdtB unfolding is not required for its exit from the ER. It is structurally feasible for HdCdtB to exit the ER in a folded state, as passage of folded proteins through the Sec61 translocon pore has been documented [48]. The translocon, which can dilate to 60Åin diameter [49], could accommodate the 45Ådiameter of an isolated, folded CdtB subunit [50]. Flexibility in the structure of CdtB [50] could also allow the folded toxin to assume a conformation suitable for passage through the Sec61p translocon or other pores in the ER membrane.

Our data further suggest that HdCdtB follows a unique translocation route involving direct passage from the ER to the nucleus. However, we cannot currently discount the possibility that HdCdtB first enters the cytosol and then rapidly moves into the nucleus through the nuclear pore complex. Atypical nuclear localization sequences in other CdtB subunits [51,52] are often used as evidence for a cytosol-to-nucleus transport route, but these sequences could also serve as retrieval motifs to return an escaped pool of toxin to the nucleus. Likewise, the KDEL motif in CT is thought to act as an ER retention motif rather than as a primary ER targeting motif [53]. Given the many unique aspects of HdCdtB translocation, we favor the ER-to-nucleus model of HdCdtB translocation and are currently working to define the molecular details of this process.

Acknowledgements

This work was supported by NIH grants K22 AI054568 and R01 AI073783 to K. Teter. T. Frisan was supported by funds from the Swedish Research Council, the Swedish Cancer Society, The Åke-Wiberg Foundation, and the Karolinska Institutet. We thank Sandra Geden for technical assistance with the in vitro farnesylation assay.

Abbreviations

CT
: cholera toxin

CD
: circular dichroism

CDT
: cytolethal distending toxin

ER

endoplasmic reticulum

ERAD
endoplasmic reticulum-associated degradation

GST
glutathione S-transferase

HdCDT
Haemophilus ducreyi cytolethal distending toxin

EC_{50}
half-maximal effective concentration

PT
pertussis toxin

References

1. Thelestam, M.; Frisan, T. Cytolethal distending toxins. In: Alouf, JE.; Popoff, MR., editors. The Comprehensive Sourcebook of Bacterial Protein Toxins. Academic Press; San Diego: 2006. p. 448-467.
2. Cortes-Bratti X, Chaves-Olarte E, Lagergard T, Thelestam M. Cellular internalization of cytolethal distending toxin from *Haemophilus ducreyi*. Infect Immun 2000;68:6903–6911. [PubMed: 11083812]
3. Guerra L, Teter K, Lilley BN, Stenerlow B, Holmes RK, Ploegh HL, Sandvig K, Thelestam M, Frisan T. Cellular internalization of cytolethal distending toxin: a new end to a known pathway. Cell Microbiol 2005;7:921–934. [PubMed: 15953025]
4. Hazes B, Read RJ. Accumulating evidence suggests that several AB-toxins subvert the endoplasmic reticulum-associated protein degradation pathway to enter target cells. Biochemistry 1997;36:11051–11054. [PubMed: 9333321]
5. Lord JM, Roberts LM, Lencer WI. Entry of protein toxins into mammalian cells by crossing the endoplasmic reticulum membrane: co-opting basic mechanisms of endoplasmic reticulum-associated degradation. Curr Top Microbiol Immunol 2005;300:149–168. [PubMed: 16573240]
6. Geden SE, Gardner RA, Fabbrini MS, Ohashi M, Phanstiel O IV, Teter K. Lipopolyamine treatment increases the efficacy of intoxication with saporin and an anticancer saporin conjugate. FEBS J 2007;274:4825–4836. [PubMed: 17714513]
7. Teter K, Holmes RK. Inhibition of endoplasmic reticulum-associated degradation in CHO cells resistant to cholera toxin, *Pseudomonas aeruginosa* exotoxin A, and ricin. Infect Immun 2002;70:6172–6179. [PubMed: 12379695]
8. Teter K, Jobling MG, Holmes RK. A class of mutant CHO cells resistant to cholera toxin rapidly degrades the catalytic polypeptide of cholera toxin and exhibits increased endoplasmic reticulum-associated degradation. Traffic 2003;4:232–242. [PubMed: 12694562]
9. Navarro-Garcia F, Canizalez-Roman A, Burlingame KE, Teter K, Vidal JE. Pet, a non-AB toxin, is transported and translocated into epithelial cells by a retrograde trafficking pathway. Infect Immun 2007;75:2101–2109. [PubMed: 17296748]
10. Argent RH, Parrott AM, Day PJ, Roberts LM, Stockley PG, Lord JM, Radford SE. Ribosome-mediated folding of partially unfolded ricin A-chain. J Biol Chem 2000;275:9263–9269. [PubMed: 10734065]
11. Pande AH, Moe D, Jamnadas M, Tatulian SA, Teter K. The pertussis toxin S1 subunit is a thermally unstable protein susceptible to degradation by the 20S proteasome. Biochemistry 2006;45:13734–13740. [PubMed: 17105192]
12. Pande AH, Scaglione P, Taylor M, Nemec KN, Tuthill S, Moe D, Holmes RK, Tatulian SA, Teter K. Conformational instability of the cholera toxin A1 polypeptide. J Mol Biol 2007;374:1114–1128. [PubMed: 17976649]

13. Goins B, Freire E. Thermal stability and intersubunit interactions of cholera toxin in solution and in association with its cell-surface receptor ganglioside GM1. Biochemistry 1988;27:2046–2052. [PubMed: 3378043]

14. Krell T, Greco F, Nicolai MC, Dubayle J, Renauld-Mongenie G, Poisson N, Bernard I. The use of microcalorimetry to characterize tetanus neurotoxin, pertussis toxin and filamentous haemagglutinin. Biotechnol Appl Biochem 2003;38:241–251. [PubMed: 12911336]

15. Jackson LS, Tolleson WH, Chirtel SJ. Thermal inactivation of ricin using infant formula as a food matrix. J Agric Food Chem 2006;54:7300–7304. [PubMed: 16968097]

16. Deeks ED, Cook JP, Day PJ, Smith DC, Roberts LM, Lord JM. The low lysine content of ricin A chain reduces the risk of proteolytic degradation after translocation from the endoplasmic reticulum to the cytosol. Biochemistry 2002;41:3405–3413. [PubMed: 11876649]

17. Frisan T, Cortes-Bratti X, Chaves-Olarte E, Stenerlow B, Thelestam M. The *Haemophilus ducreyi* cytolethal distending toxin induces DNA double-strand breaks and promotes ATM-dependent activation of RhoA. Cell Microbiol 2003;5:695–707. [PubMed: 12969375]

18. Li L, Sharipo A, Chaves-Olarte E, Masucci MG, Levitsky V, Thelestam M, Frisan T. The *Haemophilus ducreyi* cytolethal distending toxin activates sensors of DNA damage and repair complexes in proliferating and non-proliferating cells. Cell Microbiol 2002;4:87–99. [PubMed: 11896765]

19. Teter K, Allyn RL, Jobling MG, Holmes RK. Transfer of the cholera toxin A1 polypeptide from the endoplasmic reticulum to the cytosol is a rapid process facilitated by the endoplasmic reticulum-associated degradation pathway. Infect Immun 2002;70:6166–6171. [PubMed: 12379694]

20. Cope LD, Lumbley S, Latimer JL, Klesney-Tait J, Stevens MK, Johnson LS, Purven M, Munson RS Jr, Lagergard T, Radolf JD, Hansen EJ. A diffusible cytotoxin of *Haemophilus ducreyi*. Proc Natl Acad Sci USA 1997;94:4056–4061. [PubMed: 9108104]

21. Nesic D, Hsu Y, Stebbins CE. Assembly and function of a bacterial genotoxin. Nature 2004;429:429–433. [PubMed: 15164065]

22. Wu MM, Llopis J, Adams SR, McCaffery JM, Teter K, Kulomaa MS, Machen TE, Moore HP, Tsien RY. Studying organelle physiology with fusion protein-targeted avidin and fluorescent biotin conjugates. Methods Enzymol 2000;327:546–564. [PubMed: 11045008]

23. Barrero MJ, Montero M, Alvarez J. Dynamics of [Ca2+] in the endoplasmic reticulum and cytoplasm of intact HeLa cells. A comparative study. J Biol Chem 1997;272:27694–27699. [PubMed: 9346910]

24. Kim JH, Johannes L, Goud B, Antony C, Lingwood CA, Daneman R, Grinstein S. Noninvasive measurement of the pH of the endoplasmic reticulum at rest and during calcium release. Proc Natl Acad Sci USA 1998;95:2997–3002. [PubMed: 9501204]

25. Hofer AM, Schulz I. Quantification of intraluminal free [Ca] in the agonist-sensitive internal calcium store using compartmentalized fluorescent indicators: some considerations. Cell Calcium 1996;20:235–242. [PubMed: 8894270]

26. Tsai B, Rodighiero C, Lencer WI, Rapoport TA. Protein disulfide isomerase acts as a redox-dependent chaperone to unfold cholera toxin. Cell 2001;104:937–948. [PubMed: 11290330]

27. Bark SJ, Muster N, Yates JR 3rd, Siuzdak G. High-temperature protein mass mapping using a thermophilic protease. J Am Chem Soc 2001;123:1774–1775. [PubMed: 11456785]

28. Renn JP, Clark PL. A conserved stable core structure in the passenger domain beta-helix of autotransporter virulence proteins. Biopolymers 2008;89:420–427. [PubMed: 18189304]

29. Orlandi PA. Protein-disulfide isomerase-mediated reduction of the A subunit of cholera toxin in a human intestinal cell line. J Biol Chem 1997;272:4591–4599. [PubMed: 9020187]

30. Coux O, Tanaka K, Goldberg AL. Structure and functions of the 20S and 26S proteasomes. Annu Rev Biochem 1996;65:801–847. [PubMed: 8811196]

31. Romisch K. A cure for traffic jams: small molecule chaperones in the endoplasmic reticulum. Traffic 2004;5:815–820. [PubMed: 15479447]

32. Sandvig K, Madshus IH, Olsnes S. Dimethyl sulphoxide protects cells against polypeptide toxins and poliovirus. Biochem J 1984;219:935–940. [PubMed: 6331401]

33. Scaglione P, Nemec KN, Burlingame KE, Grabon A, Huerta J, Navarro-Garcia F, Tatulian SA, Teter K. Structural characteristics of the plasmid-encoded toxin from enteroaggregative *Escherichia coli*. Biochemistry 2008;47:9582–9591. [PubMed: 18702515]

34. Clarke S. Protein isoprenylation and methylation at carboxyl-terminal cysteine residues. Annu Rev Biochem 1992;61:355–386. [PubMed: 1497315]
35. Fricker M, Hollinshead M, White N, Vaux D. Interphase nuclei of many mammalian cell types contain deep, dynamic, tubular membrane-bound invaginations of the nuclear envelope. J Cell Biol 1997;136:531–544. [PubMed: 9024685]
36. Echevarria W, Leite MF, Guerra MT, Zipfel WR, Nathanson MH. Regulation of calcium signals in the nucleus by a nucleoplasmic reticulum. Nat Cell Biol 2003;5:440–446. [PubMed: 12717445]
37. Lagace TA, Ridgway ND. The rate-limiting enzyme in phosphatidylcholine synthesis regulates proliferation of the nucleoplasmic reticulum. Mol Biol Cell 2005;16:1120–1130. [PubMed: 15635091]
38. Majoul IV, Bastiaens PI, Soling HD. Transport of an external Lys-Asp-Glu-Leu (KDEL) protein from the plasma membrane to the endoplasmic reticulum: studies with cholera toxin in Vero cells. J Cell Biol 1996;133:777–789. [PubMed: 8666663]
39. Johannes L, Tenza D, Antony C, Goud B. Retrograde transport of KDEL-bearing B-fragment of Shiga toxin. J Biol Chem 1997;272:19554–19561. [PubMed: 9235960]
40. Castro MG, McNamara U, Carbonetti NH. Expression, activity and cytotoxicity of pertussis toxin S1 subunit in transfected mammalian cells. Cell Microbiol 2001;3:45–54. [PubMed: 11207619]
41. Spano S, Ugalde JE, Galan JE. Delivery of a *Salmonella* Typhi exotoxin from a host intracellular compartment. Cell Host Microbe 2008;3:30–38. [PubMed: 18191792]
42. Deng K, Latimer JL, Lewis DA, Hansen EJ. Investigation of the interaction among the components of the cytolethal distending toxin of *Haemophilus ducreyi*. Biochem Biophys Res Commun 2001;285:609–615. [PubMed: 11453636]
43. Lee RB, Hassane DC, Cottle DL, Pickett CL. Interactions of *Campylobacter jejuni* cytolethal distending toxin subunits CdtA and CdtC with HeLa cells. Infect Immun 2003;71:4883–4890. [PubMed: 12933829]
44. Mao X, DiRienzo JM. Functional studies of the recombinant subunits of a cytolethal distending holotoxin. Cell Microbiol 2002;4:245–255. [PubMed: 11952641]
45. Akifusa S, Heywood W, Nair SP, Stenbeck G, Henderson B. Mechanism of internalization of the cytolethal distending toxin of *Actinobacillus actinomycetemcomitans*. Microbiology 2005;151:1395–1402. [PubMed: 15870449]
46. Lara-Tejero M, Galan JE. CdtA, CdtB, and CdtC form a tripartite complex that is required for cytolethal distending toxin activity. Infect Immun 2001;69:4358–4365. [PubMed: 11401974]
47. Boesze-Battaglia K, Besack D, McKay T, Zekavat A, Otis L, Jordan-Sciutto K, Shenker BJ. Cholesterol-rich membrane microdomains mediate cell cycle arrest induced by *Actinobacillus actinomycetemcomitans* cytolethal-distending toxin. Cell Microbiol 2006;8:823–836. [PubMed: 16611231]
48. Fiebiger E, Story C, Ploegh HL, Tortorella D. Visualization of the ER-to-cytosol dislocation reaction of a type I membrane protein. EMBO J 2002;21:1041–1053. [PubMed: 11867532]
49. Hamman BD, Chen JC, Johnson EE, Johnson AE. The aqueous pore through the translocon has a diameter of 40–60 A during cotranslational protein translocation at the ER membrane. Cell 1997;89:535–544. [PubMed: 9160745]
50. Hontz JS, Villar-Lecumberri MT, Potter BM, Yoder MD, Dreyfus LA, Laity JH. Differences in crystal and solution structures of the cytolethal distending toxin B subunit: Relevance to nuclear translocation and functional activation. J Biol Chem 2006;281:25365–25372. [PubMed: 16809347]
51. McSweeney LA, Dreyfus LA. Nuclear localization of the *Escherichia coli* cytolethal distending toxin CdtB subunit. Cell Microbiol 2004;6:447–458. [PubMed: 15056215]
52. Nishikubo S, Ohara M, Ueno Y, Ikura M, Kurihara H, Komatsuzawa H, Oswald E, Sugai M. An N-terminal segment of the active component of the bacterial genotoxin cytolethal distending toxin B (CDTB) directs CDTB into the nucleus. J Biol Chem 2003;278:50671–50681. [PubMed: 12947116]
53. Lencer WI, Tsai B. The intracellular voyage of cholera toxin: going retro. Trends Biochem Sci 2003;28:639–645. [PubMed: 14659695]

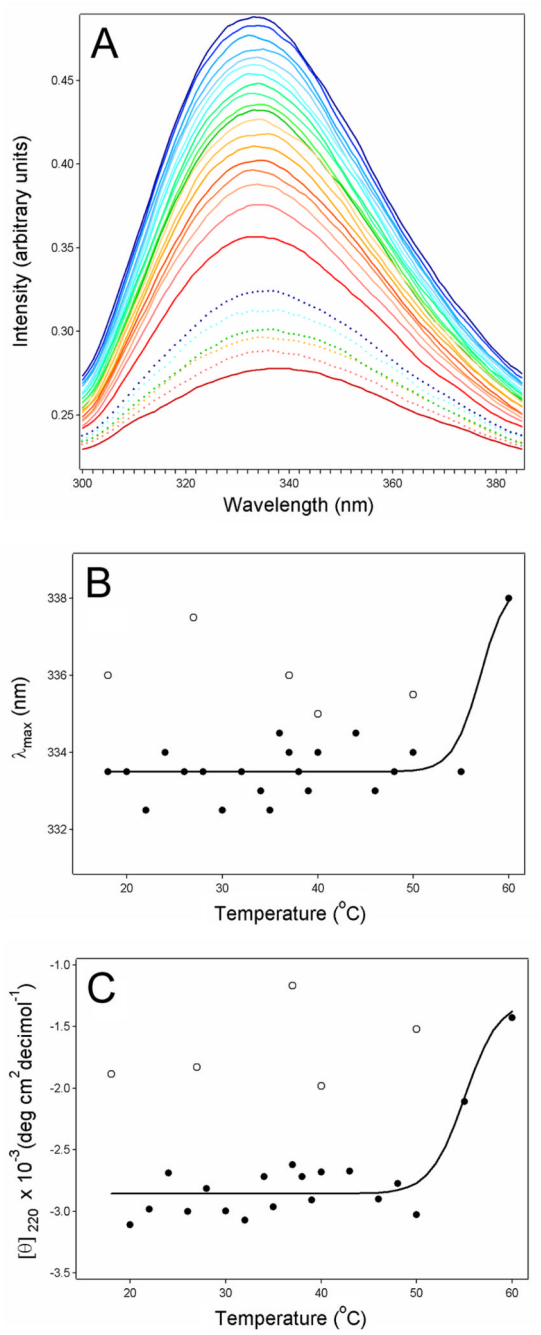

Figure 1.

HdCdtB thermal stability. Temperature-induced changes to the structure of HdCdtB were monitored by fluorescence spectroscopy (A–B) and far-UV CD (C). Both measurements were conducted near-simultaneously on the same sample after equilibration at each temperature for 3 min. Three scans per spectra were collected and averaged to improve the signal-to-noise ratio. (A): The change in color from blue to red corresponds to a stepwise increase in temperature from 18°C to 60°C. Dotted lines are spectra of samples cooled to 50°C, 40°C, 37°C, 25°C, and 18°C after HdCdtB was heated to 60°C; colors indicate the same temperatures as the solid lines. (B): The maximum emission wavelengths (λ_{max}) from panel A were plotted as a function of temperature. Data points from the cooled HdCdtB spectra are presented as

open circles. (C): For far-UV CD analysis, the mean residue molar ellipticities at 220 nm ($[\theta]_{220}$) were plotted as a function of temperature. Data points from the cooled HdCdtB spectra are presented as open circles. The solid lines in panels B and C are best fit curves simulated as described in Ref. [11].

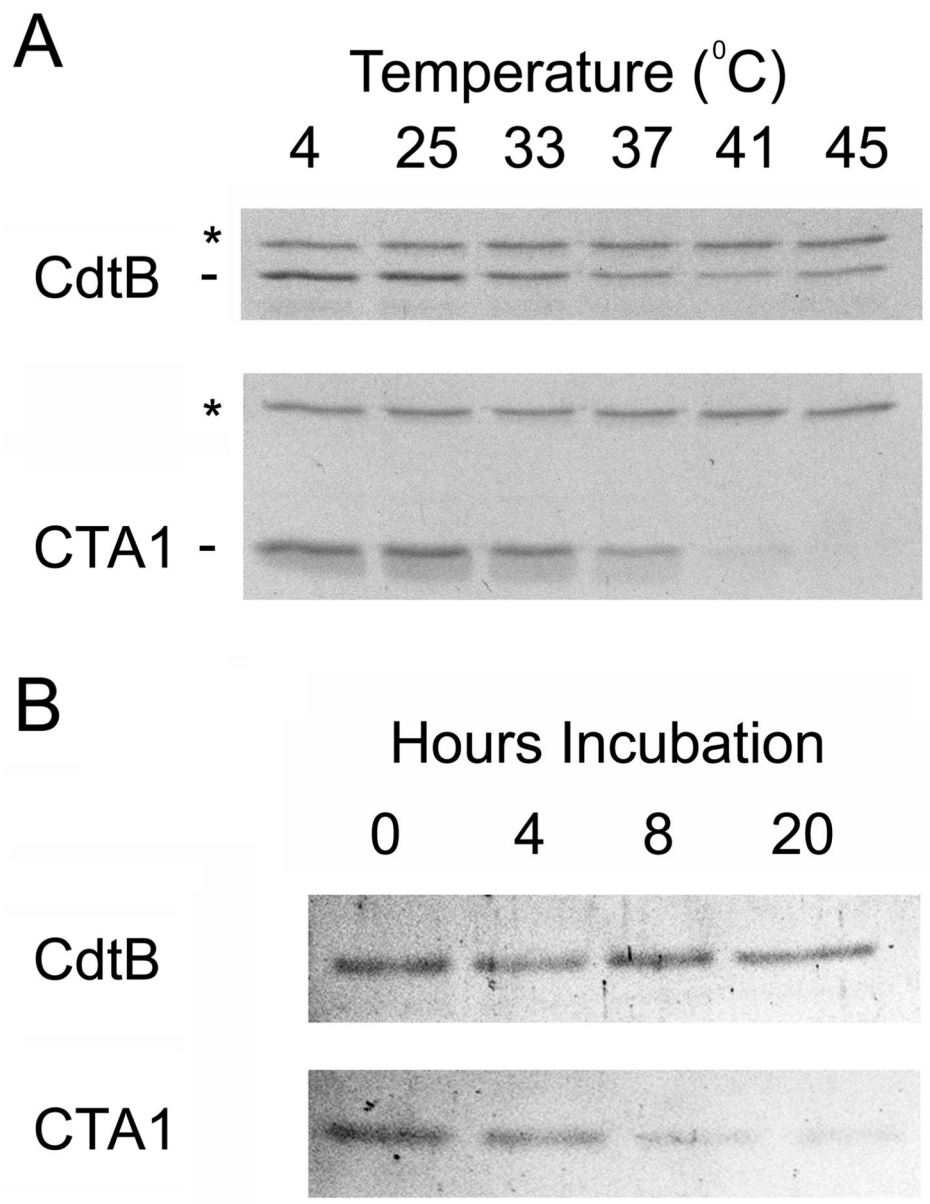

Figure 2.

HdCdtB proteolysis. (A): HdCdtB or the CTA1/CTA2 heterodimer was placed in 20 mM Na-phosphate buffer (pH 7.0) containing 10 mM β-mercaptoethanol. After incubation at the indicated temperatures for 45 min, thermolysin was added for an additional 45 min at 4ºC. Proteolysis was halted by the addition of EDTA and sample buffer. The toxins were then visualized by SDS-PAGE and Coomassie staining. For both gels, the upper thermolysin band is denoted with an asterisk. (B): HdCdtB or the reduced CTA1/CTA2 heterodimer was placed in assay buffer with 100 nM of the 20S proteasome. Proteolysis was halted after 0, 4, 8, or 20 h of incubation at 37ºC. The toxins were then visualized by SDS-PAGE and Coomassie staining.

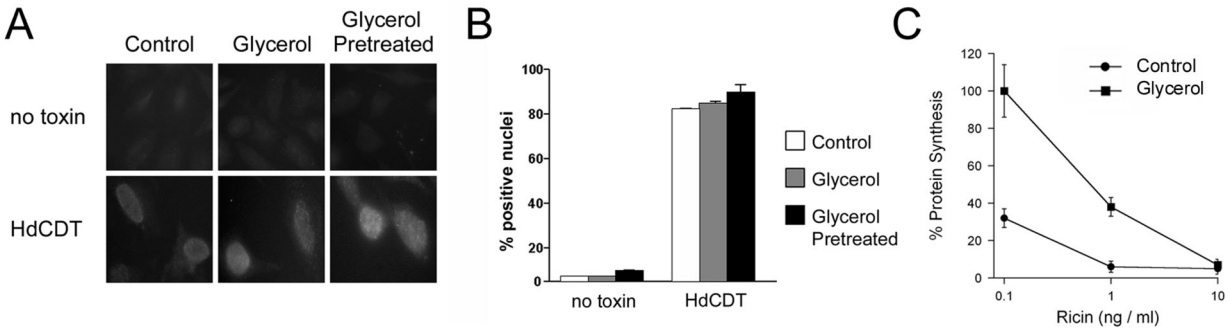

Figure 3.

HdCDT toxicity. (A–B): HeLa cells were incubated with no toxin or with 2 μg/ml of HdCDT for 2 h in medium alone (control) or medium supplemented with 10% glycerol. As indicated, one set of cells were pretreated with 10% glycerol medium for 1 hr before a further 2 h incubation with glycerol in the absence (no toxin) or presence of HdCDT. (A): Toxin-induced phosphorylation of histone H2AX was visualized in fixed cells with a rabbit anti-phospho-H2AX antibody and a FITC-conjugated swine anti-rabbit IgG antibody. One of two experiments is shown. (B): The graph charts the average percentage (± range) of nuclei positive for H2AX foci from both experiments. (C): HeLa cells were incubated with various concentrations of ricin for 4 h in the absence or presence of 10% glycerol before protein synthesis levels were quantified. Measurements taken from unintoxicated cells incubated in the absence or presence of glycerol were used to establish the 100% value for the corresponding experimental condition. The average ± range of two independent experiments with triplicate samples is shown.

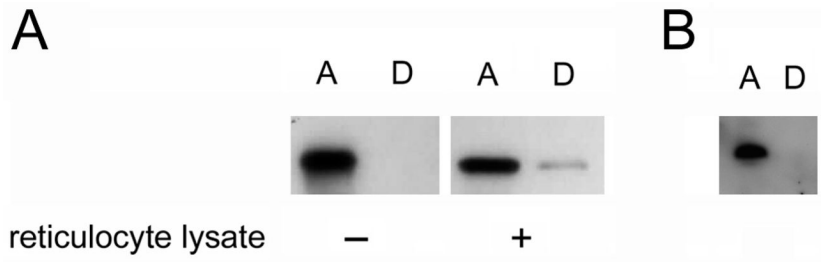

Figure 4.

HdCdtB translocation. (A): Purified GST-HdCdtB-CVIM was incubated in the absence or presence of rabbit reticulocyte lysate before placement in cold 1% Triton X-114. Aqueous (A) and detergent (D) phases of Triton X-114 were isolated by centrifugation of the warmed samples. The distribution of GST-HdCdtB-CVIM was then determined by Western blot analysis of the separate detergent and aqueous phases. (B): For in vivo farnesylation of GST-HdCdtB-CVIM, HeLa cells were exposed for 4 h to 50μg/ml of a recombinant CDT holotoxin that contained the GST-HdCdtB-CVIM subunit. After lysis in 1% Triton X-114, aqueous (A) and detergent (D) phases were separated. GST-HdCdtB-CVIM was recovered by affinity purification and visualized by Western-blot analysis as described in Materials and methods.

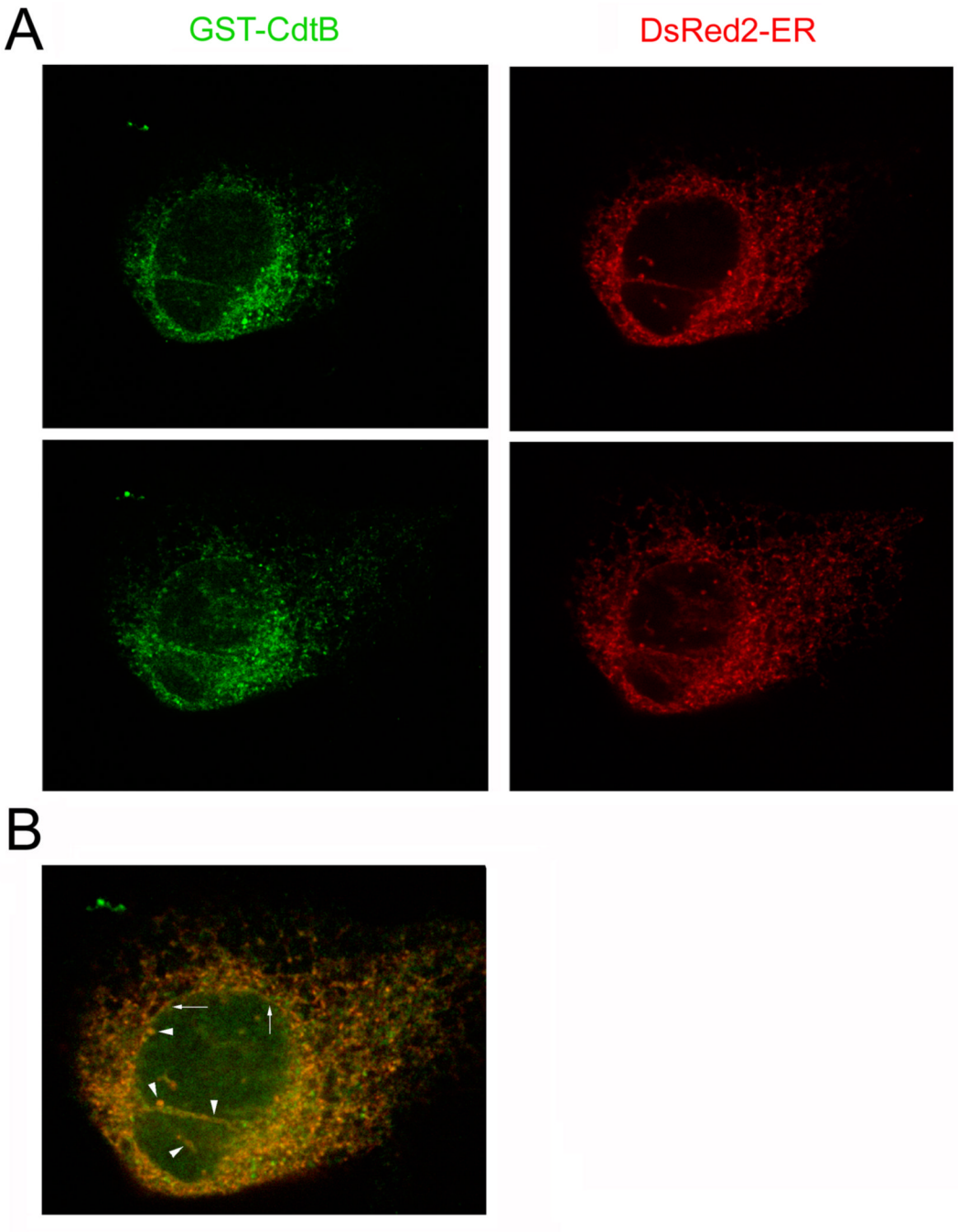

Figure 5.
Intracellular distribution of HdCdtB. Transfected HeLa cells expressing DsRed2-ER, a fluorescent marker for the ER, were exposed for 4 h to 10 μg/ml of a recombinant CDT holotoxin that contained a GST-HdCdtB subunit. The cells were then fixed and stained with a fluorescein-conjugated anti-GST antibody. (A): Labeling patterns for DsRed2-ER and GST-CdtB from two Z-sections of a single cell. (B): The merged image of DsRed2-ER and GST-CdtB distributions. Arrows denote the nuclear envelope; arrowheads denote invaginations of the nucleoplasmic reticulum.